Yunqing Ma[a,b], Lihong Xu[a], Yan Li[a], Chengbao Jiang[a], Huibin Xu[a], Young-Kook Lee[b]
[a] Department of Materials Science and Engineering, Beijing University of Aeronautics and Astronautics, Beijing, P.R. China
[b] Department of Metallurgical Engineering, Yonsei University, Seoul, Korea

Martensitic transformation, ductility, and shape-memory effect of polycrystalline $Ni_{56}Mn_{25-x}Fe_xGa_{19}$ alloys

Buttons of high-temperature shape-memory alloy $Ni_{56}Mn_{25-x}Fe_xGa_{19}$ were prepared by arc melting under argon atmosphere. The specimens were hot rolled to 1 mm plates, and their martensitic transformation behaviors, ductilities, and shape-memory effects were investigated through differential scanning calorimetry and bending tests. It was found that the brittleness of polycrystalline Ni_2MnGa was ameliorated through introduction of a ductile phase by Fe addition. $Ni_{56}Mn_{17}Fe_8Ga_{19}$ alloy shows great potential as a practical high-temperature shape-memory alloy with martensitc transformation start temperature above 200 °C. It can bear strain of 6 % before fracture in bending tests and shows a maximum reversible strain of 3.5 %.

Keywords: NiMnGa Heusler alloy; High temperature shape-memory effect; Ductility; Martensitic transformation

1. Introduction

Although high-temperature shape-memory alloys (HTSMAs) have been shown to be an interesting and important research subject for nearly three decades [1, 2], some problems still remain unsolved in the HTSMAs reported up to date. For instance, Cu-based and NiAl HTSMAs are considered unstable [3, 4] because equilibrium phases detrimental to the shape-memory effect (SME) precipitate at high temperatures. NiTiZr and NiTiHf HTSMAs are too brittle for practical use [5]. As regards the NiTiPd alloy, although its full recovery strain has been increased to 5.5 % by proper thermomechanical treatment [6], the high cost of Pd hinders its real application. The studies to explore low-cost HTSMAs keep active.

Recently, Ni_2MnGa Heusler alloys, which possess a bcc $L2_1$ structure at high temperature and undergo a martensitic transformation to a complex tetragonal structure upon cooling, have been extensively explored as actuator materials [7–9]. Several papers [10, 11] revealed that a high martensitic transformation temperature (up to 350 °C) exists in NiMnGa alloys with Ni content higher than the stoichiometric Ni2MnGa. However, such alloys exhibit low Curie temperatures and saturation magnetizations, and therefore show little potential as magnetic shape-memory alloys.

Our previous work revealed that single crystalline $Ni_{54}Mn_{25}Ga_{21}$ exhibits a large reversible strain (6.1 %) and a high martensitic transformation start temperature (Ms > 200 °C), and that 1000 thermal cycles have little influence on the microstructure, the martensitic transformation behavior, as well as on its shape-memory effect [12]. This good thermal stability is thought to result from the high degree of the self-accommodation of martensitic variants [13]. All these make the NiMnGa alloy a promising HTSMA. However, the brittleness of polycrystalline NiMnGa ternary alloys is a vital obstacle to practical applications.

Therefore, this study was carried out to develop a ductile polycrystalline HTSMA by adding Fe to the NiMnGa ternary system. The addition of Fe is expected to introduce a ductile fcc phase into the brittle NiMnGa alloys, leading to an improvement in ductility while keeping a good shape-memory ability.

2. Experimental

$Ni_{56}Mn_{25-x}Fe_xGa_{19}$ (x = 0, 4, 8, 12, 16 in atomic percent) polycrystals were prepared by melting relatively pure metals (99.9 %) under argon atmosphere using an arc melter. Each specimen of about 50 g was remelted four times followed by homogenization at 800 °C for 4 days in a sealed quartz ampoule. The specimens were hot-rolled to make thin plates of 1 mm thickness, which were heated at 800 °C for 30 min followed by quench into water. The microstructures were identified at room temperature by X-ray diffraction tests (Rigaku D/Max 2200 PC diffractometer with Cu–Ka radiation). The phase transformation temperatures of the alloys were determined by differential scanning calorimetry (DSC) (NETZSCH STA449) at cooling and heating rates of 10 K/min.

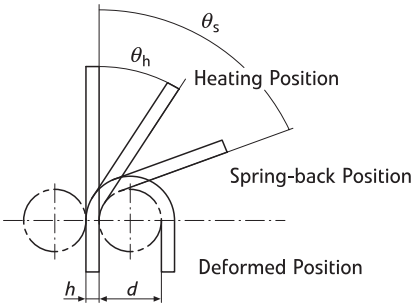

Fig. 1. Schematic illustration of the bending test for the SME measurement.

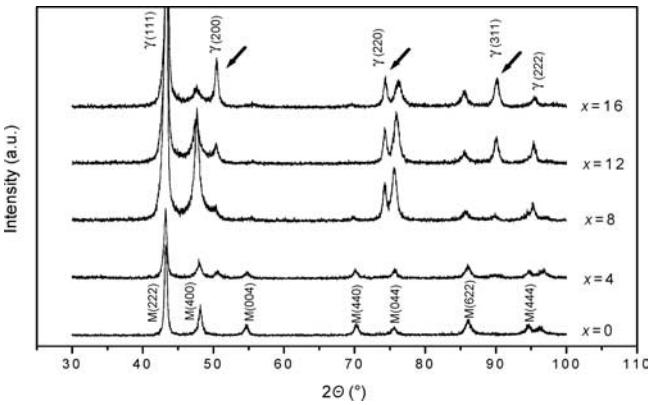

Fig. 2. X-ray diffraction patterns of $Ni_{56}Mn_{25-x}Fe_xGa_{19}$ alloys measured at room temperature.

The specimens of $1 \times 2 \times 50$ mm^3 were cut in the rolling direction from the heat-treated plates, and their SME was examined by bending tests, as schematically shown in Fig. 1 [14]. One end of the SME sample was clipped at the center of the plate. The specimen was deformed at room temperature, and then heated up to 400 °C for shape recovery. The pre-strain, $\varepsilon = h/(d + h)$, is about 5.5 % in the present study, and the recovery ratio was calculated as $R = (\theta_d - \theta_h)/\theta_d$.

3. Results and discussion

3.1. Microstructure and phase transformation behavior

Figure 2 shows the X-ray diffraction patterns of $Ni_{56}Mn_{25-x}Fe_xGa_{19}$ ($x = 0$, 4, 8, 12, 16) alloys measured at room temperature. The $Ni_{56}Mn_{25}Ga_{19}$ ternary alloy ($x = 0$) shows typical non-modulated tetragonal martensite (denoted as M), which is the same as previously reported in several references [15–17]. No other phases were detected in the Fe-free specimen. The $Ni_{56}Mn_{25-x}Fe_xGa_{19}$ alloys show additional diffraction peaks, as indicated by the arrows in Fig. 2. The intensities of the additional peaks increased with increasing Fe content, while their positions were almost unchanged, which implies that a new phase was formed by the addition of Fe, and the amount of the new phase increased with increasing Fe content. The new phase was confirmed as γ (face-centered cubic) phase with the main diffraction peaks of (111), (200), (220), (311), and (222), as shown in Fig. 2. Among the γ peaks, γ(111) and γ(222) peaks overlap with M(222) and M(444) peaks, respectively. The lattice parameter of the γ phase is $a = 3.620$ Å.

Light-optical micrographs of $Ni_{56}Mn_{25-x}Fe_xGa_{19}$ alloys are shown in Fig. 3. In accordance with the X-ray diffraction results, the $Ni_{56}Mn_{25}Ga_{19}$ alloy (Fig. 3a) exhibits a typical martensite structure with different variants. The interfaces between the martensite variants are straight and clear. When 4 at.% Fe is added, (Fig. 3b), a new phase with a granular shape appeared at the boundaries of variants and grains. The appearance of these granules is in good agreement with the X-ray diffraction results, implying that the second phase must be the γ phase. With the increase in Fe content, the amount and the size of γ phase increased gradually. When Fe increased to 12 at.% (Fig. 3d) and to 16 at.% (Fig. 3e), the γ phase is connected forming a dendritic framework, and the martensite variants become obscure to be distinguished. The γ phase does not participate in the reversible martensitic transformation [18, 19], and its size, shape, and distribution possibly have effects on the martensitic transformation and the reorientation of martensitic variants.

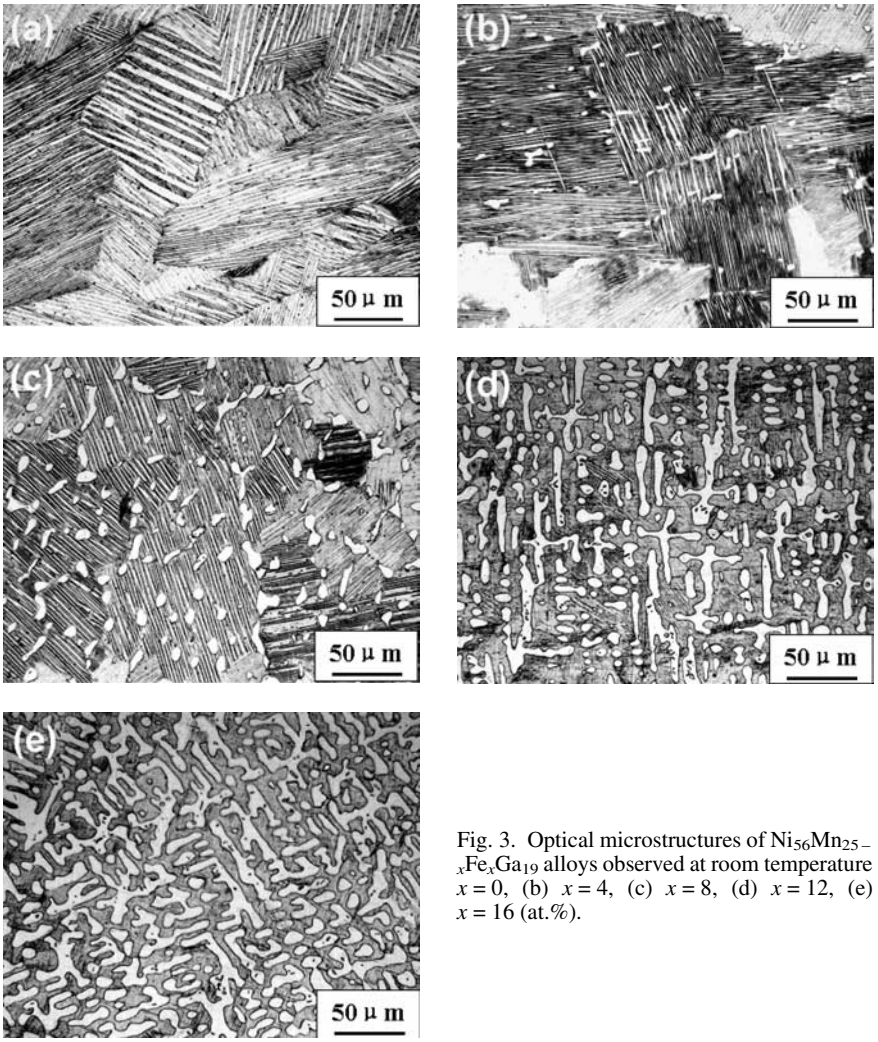

Fig. 3. Optical microstructures of $Ni_{56}Mn_{25-x}Fe_xGa_{19}$ alloys observed at room temperature $x = 0$, (b) $x = 4$, (c) $x = 8$, (d) $x = 12$, (e) $x = 16$ (at.%).

Table 1 summarizes the compositions, martensitic transformation temperatures and latent heats of $Ni_{56}Mn_{25-x}Fe_xGa_{19}$ alloys. *Mp* denotes the peak temperature of martensitic transformation during cooling and *Ap* the peak temperature of the reverse transformation during heating, and the hysteresis is the temperature interval between *Ap* and *Mp*. The addition of Fe decreases the martensitic transformation temperatures (*Ap* and *Mp*) of $Ni_{56}Mn_{25-x}Fe_xGa_{19}$ alloys.

Table 1. Martensitic transformation temperatures and the latent heats of $Ni_{56}Mn_{25-x}Fe_xGa_{19}$ alloys.

Sample (at.%)	*Ap* (°C)	*Mp* (°C)	Hysteresis (K)	$\Delta H_{M\to A}$ (J/g)	$\Delta H_{A\to M}$ (J/g)
$Ni_{56}Mn_{25}Ga_{19}$	452.4	400.9	51.5	9.8	12.3
$Ni_{56}Mn_{21}Fe_4Ga_{19}$	385.0	339.8	45.2	6.1	6.2
$Ni_{56}Mn_{17}Fe_8Ga_{19}$	235.8	216.3	19.5	4.2	5.1
$Ni_{56}Mn_{13}Fe_{12}Ga_{19}$	146.3	132.1	14.2	2.9	3.4
$Ni_{56}Mn_9Fe_{16}Ga_{19}$	90.3	80.6	9.7	2.2	2.4

When the Fe content increased from zero to 16 at.%, the *Ap* temperature decreased from 452.4 to 90.3 °C, the *Mp* temperature decreased from 400.9 to 80.6 °C, and the corresponding hysteresis decreased from 51.5 to 9.7 °C, respectively. The relationship between the martensitic transformation temperatures and the Fe content is plotted in Fig. 4. The martensitic transformation temperatures are almost linearly decreased with increasing Fe content in $Ni_{56}Mn_{25-x}Fe_xGa_{19}$ alloys.

$$Ap(°C) = 454.5 - 24.1 \times (\text{at.\% Fe})$$

$$Mp(°C) = 403.6 - 21.2 \times (\text{at.\% Fe})$$

Although the martensitic transformation temperatures decreased with Fe content in $Ni_{56}Mn_{25-x}Fe_xGa_{19}$ alloys, both *Mp* and *Ap* temperatures are still above 200 °C as long as the Fe content does not exceed 8 at.%.

The latent heats of the martensitic and reverse transformations in $Ni_{56}Mn_{25-x}Fe_xGa_{19}$ alloys reduced gradually with increasing Fe content. This resulted from the decrease in martensite amount with Fe content, as shown in Fig. 3.

3.2. Ductility and shape-memory effect

Bending tests were performed to examine the ductility of $Ni_{56}Mn_{25-x}Fe_xGa_{19}$ alloys, which was described by the maximum bending strain before fracture. The results are listed in Table 2. The ductilities of $Ni_{56}Mn_{25-x}Fe_xGa_{19}$ alloys increased with the Fe content, indicating that the amount of γ phase plays an important role in improving the ductility. The $Ni_{56}Mn_{25}Ga_{19}$ and $Ni_{56}Mn_{21}Fe_4Ga_{19}$ alloys could not be hot-rolled to plates of 1 mm thickness due to their brittleness. The $Ni_{56}Mn_9Fe_{16}Ga_{19}$ alloy, having the greatest amount of γ phase, bear over 14 % strain before fracture. But its peak martensitic transformation temperature (*Mp*) is as low as 80 °C, which is not satisfactory for HTSMAs [1, 2]. The $Ni_{56}Mn_{17}Fe_8Ga_{19}$ alloy shows a good combination of moderate ductility (over 6 % strain before fracture) and high martensitic transformation temperature (*Mp* = 216.3 °C).

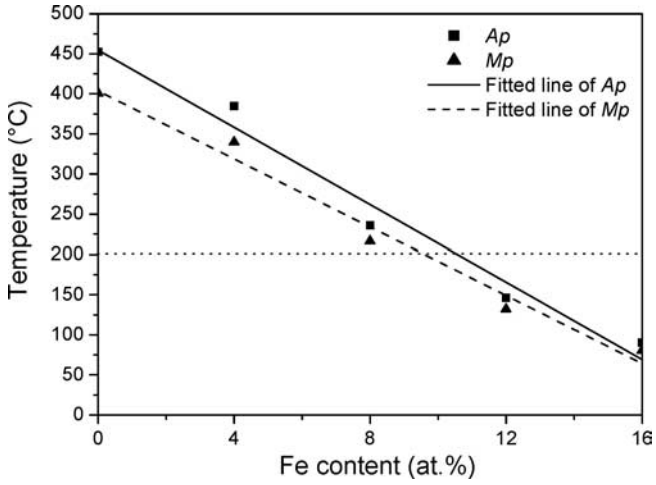

Fig. 4. Relationship between martensitic transformation temperatures and Fe contents in $Ni_{56}Mn_{25-x}Fe_xGa_{19}$ alloys.

Table 2. The ductilities of $Ni_{56}Mn_{25-x}Fe_xGa_{19}$ alloys examined by bending tests.

Sample (at.%)	Maximal strain before fracture (%)	Comments
$Ni_{56}Mn_{25}Ga_{19}$	–	Could not be hot-rolled to 1 mm
$Ni_{56}Mn_{21}Fe_4Ga_{19}$	–	Could not be hot-rolled to 1 mm
$Ni_{56}Mn_{17}Fe_8Ga_{19}$	6	
$Ni_{56}Mn_{13}Fe_{12}Ga_{19}$	9	
$Ni_{56}Mn_9Fe_{16}Ga_{19}$	14	

Table 3. The shape-memory properties of $Ni_{56}Mn_{25-x}Fe_xGa_{19}$ alloys.

Sample (at.%)	Pre-strain (%)	Recovery ratio (%)	SME strain (%)
$Ni_{56}Mn_{25}Ga_{19}$	–	–	–
$Ni_{56}Mn_{21}Fe_4Ga_{19}$	–	–	–
$Ni_{56}Mn_{17}Fe_8Ga_{19}$	5.5	64.3	3.5
$Ni_{56}Mn_{13}Fe_{12}Ga_{19}$	5.8	38.5	2.2
$Ni_{56}Mn_9Fe_{16}Ga_{19}$	5.1	29.5	1.5

Consequently, the addition of Fe brings a dramatic improvement of NiMnGa polycrystals in hot workability and room-temperature ductility due to the formation of the γ phase.

The SME of $Ni_{56}Mn_{25-x}Fe_xGa_{19}$ alloys was also examined by bending tests, and the results are shown in Table 3. The SME of the alloys decreased with increasing Fe content, because the addition of Fe introduces and increases the amount of γ phase, which does not participate in the reversible martensitic transformation, and hampers the reorientation of martensitic variants.

The $Ni_{56}Mn_{17}Fe_8Ga_{19}$ alloy exhibits good reversible strain of 3.5 %, moderate hot workability, ductility, and high martensitic transformation temperature (*Mp* = 216.3 °C).

4. Conclusions

(1) The martensitic transformation temperatures of $Ni_{56}Mn_{25-x}Fe_xGa_{19}$ alloys gradually decreased with increasing Fe content. But the martensitic transformation temperatures of $Ni_{56}Mn_{17}Fe_8Ga_{19}$ are still over 200 °C, which is good enough for HTSMA.

(2) The ductility of NiMnGa polycrystals could be improved by introducing γ phase by the addition of Fe, while keeping their shape-memory abilities.

(3) The $Ni_{56}Mn_{17}Fe_8Ga_{19}$ alloy exhibits great possibility to develop as a practical HTSMA. It shows high martensitic transformation temperature (Mp = 216.3 °C), moderate ductility (6 % strain before fracture), and a good reversible strain of 3.5 %.

The authors are grateful to Prof. Chong-Sool Choi for useful discussions and helpful advices. Financial supports from National Natural Science Foundation of China (NSFC), No. 50371005 and Yonsei University are acknowledged.

References

[1] K. Otsuka, X.B. Ren: Intermetallics 7 (1999) 511.
[2] J. Van Humbeeck: J. Eng. Mater. Tech. 121 (1999) 98.
[3] H.B. Xu: Mater. Sci. Forum 394–395 (2002) 375.
[4] J.H. Yang, C.M. Wayman: Intermetallics 2 (1994) 111.
[5] J.H. Mulder, J.H. Maas, J. Beyer: Proc. ICOMAT-92 Monterey (1992) 869.
[6] D. Golberg, Ya Xu, Y. Murakami, S. Morito, K. Otsuka: Scripta Metall. Mater. 30 (1994) 1349.
[7] K. Ullakko, J.K. Huang, C. Kantner, R.C. O'Handley, V.V. Kokorin: Appl. Phys. Lett. 69 (1996) 1966.
[8] A. Sozinov, A.A. Likhachev, N. Lanska, K. Ullakko: Appl. Phys. Lett. 80 (2002) 1746.
[9] R. Tickle, R.D. James: J. Magn. Magn. Mater. 195 (1999) 627.
[10] V.A. Chernenko, E. Cesari, V.V. Kokorin, I.N. Vitenko: Scripta Metall. Mater. 33 (1995) 1239.
[11] X. Jin, M. Marioni, D. Bono, S.M. Allen, R.C. O'Handley, T.Y. Hsu: J. Appl. Phys. 91 (2002) 8222.
[12] H.B. Xu, Y.Q. Ma, C.B. Jiang: Appl. Phys. Lett. 82 (2003) 3206.
[13] Y.Q. Ma, C.B. Jiang, G. Feng, H.B. Xu: Scripta Mater. 48 (2003) 365.
[14] X.L. Meng, Y.F. Zheng, Z. Wang, L.C. Zhao: Scripta Mater. 42 (2000) 341.
[15] S. Wirth, A. Leithe-Jasper, A.N. Vasil'ev, J.M.D. Coey: J. Magn. Magn. Mater. 167 (1997) L7.
[16] J. Pons, V.A. Chernenko, R. Santamarta, E. Cesari: Acta. Mater. 48 (2000) 3027.
[17] B. Wedel, M. Suzuki, Y. Murakami, C. Wedel, T. Suzuki, D. Shindo, K. Itagaki: J. Alloys Comp. 290 (1999) 137.
[18] K. Oikawa, T. Ota, Y. Sutou, T. Ohmori, R. Kainuma, K. Ishida: Mater. Trans. JIM 43 (2002) 2360.
[19] Y. Li, C.B. Jiang, T. Liang, Y.Q. Ma, H.B. Xu: Scripta Mater. 48 (2003) 1255.

(Received September 22, 2004; accepted January 2, 2005)

Correspondence address

Prof. Young-Kook Lee
Department of Metallurgical Engineering, Yonsei University
Shinchon-dong 134 Seodaemun-ku
Seoul 120-749, South Korea
Tel.: +82 2 2123 2831
Fax: +82 2 312 5375
E-mail: yklee@yonsei.ac.kr